A non-empirical gas slippage model for low to moderate Knudsen numbers

Shihao Wang, Alexander A. Lukyanov, Lei Wang, Yu-Shu Wu, Andrew Pomerantz, Wenyue Xu, and Robert Kleinberg

Citation: Physics of Fluids **29**, 012004 (2017); doi: 10.1063/1.4974319
View online: http://dx.doi.org/10.1063/1.4974319
View Table of Contents: http://aip.scitation.org/toc/phf/29/1
Published by the American Institute of Physics

A non-empirical gas slippage model for low to moderate Knudsen numbers

Shihao Wang,[1] Alexander A. Lukyanov,[2] Lei Wang,[1] Yu-Shu Wu,[1] Andrew Pomerantz,[2] Wenyue Xu,[2] and Robert Kleinberg[2]
[1]*Department of Petroleum Engineering, Colorado School of Mines, Golden, Colorado 80401, USA*
[2]*Schlumberger-Doll Research Center, Schlumberger, Cambridge, Massachusetts 02139, USA*

(Received 2 September 2016; accepted 6 January 2017; published online 25 January 2017)

In this study, we present a novel derivation of the gas slip flow boundary condition within micro- and nano-flow channels. The newly derived boundary condition is of second order. Our model is based on the kinetic theory of gases. The slippage condition is obtained via the calculation of the shear stress in a confined micro-channel. We have benchmarked the mass transfer rate predicted by our model with existing numerical and physical experimental data, and the new model matches experiments within 10%. *Published by AIP Publishing.* [http://dx.doi.org/10.1063/1.4974319]

INTRODUCTION

When the length scale of the flow channel is comparable to or even below the scale of the mean free path of gas, the gas becomes rarefied and the "no slip flow" boundary condition is no longer valid. In this situation, the velocity of gas molecules at the wall is higher than the velocity of the wall because a fraction of the gas molecules are diffusively reflected after hitting the wall, causing a loss of momentum. This phenomenon is typically called the "slip flow effect" or the "Knudsen effect". The near-wall region in which flow is impacted by the wall is called the Knudsen layer. Recently, Zhang *et al.*[1] and Cao *et al.*[2] thoroughly reviewed the state-of-the-art development of gas slippage models. The slip flow velocity can be expressed in the following form:

$$u_{slip} = C_1(K_N)\cdot\lambda\left(\frac{\partial u}{\partial n}\right)_s - C_2(K_N)\cdot\lambda^2\left(\frac{\partial^2 u}{\partial n^2}\right)_s \ldots. \quad (1)$$

The above formulation is used in Refs. 1 and 2 as a general form of the slippage boundary condition. In the above formulation, $u_{slip} = u_{gas} - u_{wall}$ is the velocity difference between the gas flow and the wall; K_N is the Knudsen number, defined as the ratio of gas mean free path (λ) to the characteristic length (d) of the flow pathway. For flow between two parallel plates, d is the distance between the two plates. For flow within a cylinder tube, d is the diameter of the tube. $(\partial u/\partial n)_s$ and $\left(\partial^2 u/\partial n^2\right)_s$ are the first order of flux velocity derivative and second order flux velocity derivative at the wall, respectively. C_1 and C_2 could be either constants or functions of Knudsen number, and so far no consensus on their Knudsen number dependency exits. In this work, C_1 and C_2 are expressed as functions of the Knudsen number (a constant can also be viewed as a form of function). A detailed explanation of the Knudsen number can be found in Appendix A. We restrict our work to flow through parallel plates, whose characteristic length is the distance between the two plates. If C_2 is zero, then the slippage velocity gets reduced to a first order approximation. Maxwell brought out the first-order slippage velocity formulation, in which C_1 equals to $(\sigma-2)/\sigma$, where σ is the tangential accommodation momentum coefficient (TMAC). Since then, extensive efforts have been spent on the related study of this area, as summarized by Ref. 1.

The slippage boundary condition can also be conveniently expressed by the shear stress at the wall, as follows:[4]

$$u_{slip} = A_1(K_N)\cdot\frac{\sigma-2}{\sigma}\frac{\lambda}{\mu}\tau_s - A_2(K_N)\cdot\frac{\lambda^2}{\mu}\left(\frac{\partial\tau}{\partial n}\right)_s \ldots. \quad (2)$$

In the above form, μ is the gas viscosity. And τ_s and $(\partial\tau/\partial n)_s$ are the shear stress and its first order derivative at the wall respectively. For planar geometry, Equation (2) reduces to Equation (1). Dinler *et al.*[5,6] adopt Equation (2) to investigate the impact of surface shape on the gas slippage effects.

The slippage velocity can be obtained via kinetic-based theory,[3] the Direct Simulation Monte Carlo method (DSMC),[7,8] the Lattice Boltzmann Method (LBM),[9] the Burnett or super-Burnett equation with Chapman-Enskog expansion,[10] and many other approaches. It is reported in Ref. 1 that kinetic model of Ref. 3 is the most accurate among all the existing non-empirical slip boundary models.

Accurate simulation of the Knudsen effect is of great importance to the understanding of gas flow within micro-channels. In this work, we propose an approach to calculate the slip coefficient. Our approach is based on the kinetic theory of gases. Our results could be applied to many industrial areas, such as unconventional gas flow in extremely tight formation[11] and MEMS device design.[12]

The outline of this short paper is as follows. The second section contains the derivation of the slip flow boundary conditions using elements of the kinetic theory of gases.[13] The third section describes comparison with experimental data and other existing models. At last, the paper is concluded with the summary.

SLIP VELOCITY CONDITION

There are a number of length scales to be considered in this problem: mainly, the length $1/\chi$, where χ is the

curvature of the micro-channel; σ_b is the root-mean-square surface roughness; λ is the mean free path; d is the diameter of the mirco-channel. The framework presented in this paper is valid when $1/\chi >> \sigma_b, \lambda, d$. Hence, two parallel plates are considered in this paper. On the scale of the wavelength of visible light, most surfaces are rough to different extents. The roughness cannot be simply described and is better suited for a statistical description. In this paper, two cases are considered: (a) constant rough surfaces and (b) variable rough surface.

Constant rough surface

The surfaces are assumed planar in the constant rough surface. To simplify the presentation, we concentrate on a 1D case (Figure 1). The 2D case constitutes a simple extension. We set the radial coordinate system shown in Appendix A with the origin located at point A. Consider a small volume $d\tau$ of the gas in position (r, φ, ω) inside a micro-channel confined by two smoothed parallel plates, as shown in Appendix A. In $d\tau$, the average number of collisions per unit distance is $1/\lambda$, where λ is the mean free path. According to the work of Ref. 8, for a unit area on the wall, the number of molecules in unit time that collide in $d\tau$, leave $d\tau$, and reach the area without any other collisions is

$$dN = \frac{\bar{\nu} n \cdot d\tau}{\lambda} \frac{\cos\varphi}{4\pi r^2} \exp\left(-\frac{r}{\lambda}\right). \tag{3}$$

In the above equation, $\exp(-r/\lambda)$ denotes the probability of the gas molecules collision, $\bar{\nu}$ is the average velocity of gas molecule, and $\cos\varphi/\left(4\pi r^2\right)$ is the fraction of gas molecules that finally reach the area. Using the above approach, it can be proven that the viscosity of ideal gas is $\mu = mn\bar{\nu}\lambda/3$.[14]

Consider the laminar flow between two infinitely long parallel plane walls along x direction, as shown in Figure 1. In such a case, the bulk (apparent) flow velocity u will be parallel to the walls and is only the function of the coordinate in z direction, expressed as $u(z)$. Therefore, the horizontal momentum carried by molecules from the small volume in Equation (3) is

$$dM = u(z) \cdot dN = u(z) \cdot \frac{\bar{\nu} n \cdot d\tau}{\lambda} \frac{\cos\varphi}{4\pi r^2} \exp\left(-\frac{r}{\lambda}\right). \tag{4}$$

The molecules impinging into the area on the wall can be divided into two types.

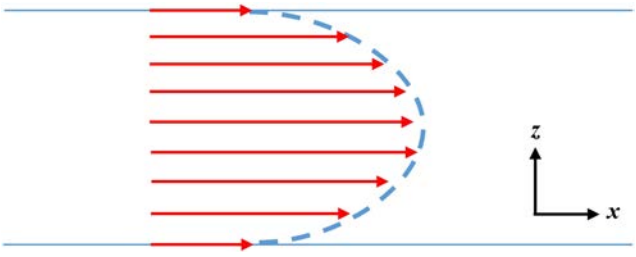

FIG. 1. Conceptual model of the laminar (shear) flow with slippage boundary. Red arrows denote horizontal flux velocity.

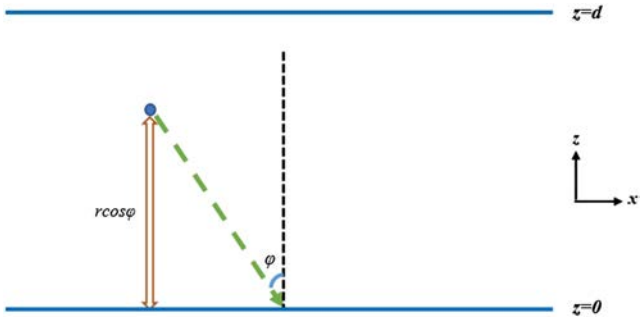

FIG. 2. Coordinates of type 1 molecules.

Type 1 molecules impinge into the plain from above after a molecular collision only and without any wall collision. The coordinates of *Type* 1 molecules within the radial coordinate system are shown in by Figure 2.

The momentum carried by these molecules is

$$M_{up} = \frac{\bar{\nu} mn}{4\pi\lambda} \int_0^{2\pi} \int_0^{\pi/2} \int_0^{l_1} u(r\cos\varphi) \cos\varphi \sin\varphi \exp(-r/\lambda)\, dr d\varphi d\omega, \tag{5}$$

where the upper limit of the distance is

$$l_1 = \frac{d}{\cos\varphi}. \tag{6}$$

The momentum can be expanded to the second order with respect to the flux velocity as

$$M_{up} \approx \frac{\bar{\nu} mn}{4\pi\lambda} \int_0^{2\pi} \int_0^{\pi/2} \int_0^{l_1} \left[u(0) + r\cos\varphi \left(\frac{du}{dz}|_{z=0}\right) + \frac{1}{2} r^2 \cos^2\varphi \left(\frac{d^2u}{dz^2}|_{z=0}\right) \right] \cos\varphi \sin\varphi \times \exp(-r/\lambda)\, dr d\varphi d\omega. \tag{7}$$

Type 2 molecules impinge into the plain after hitting the upper wall of the micro-channel. During the collision, the portion of lost momentum is σ due to the diffusive reflection (scattered). Therefore, $(1 - \sigma)$ of the total *Type* 2 molecules keep their original flux velocity as well as the flux momentum (obeying the law of reflection). This result is due to the real surfaces exhibiting some residual surface roughness. The coordinate of *Type* 2 molecules is shown in Figure 3.

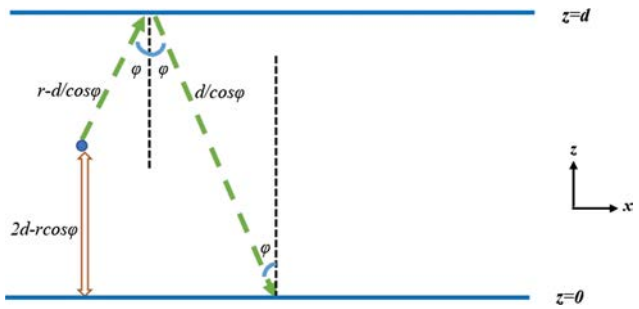

FIG. 3. Coordinates of type 2 molecules.

The momentum carried by these molecules is

$$W_{up} = (1-\sigma)\frac{\bar{v}mn}{4\pi\lambda}\int_0^{2\pi}\int_0^{\pi/2}\int_{l_1}^{l_2} u(2d - r\cos\varphi)\cos\varphi\sin\varphi\exp(-r/\lambda)\,drd\varphi d\omega, \tag{8}$$

in which

$$l_2 = \frac{2d}{\cos\varphi}. \tag{9}$$

The momentum can be expanded to the second order with respect to the flux velocity as

$$W_{up} \approx (1-\sigma)\frac{\bar{v}mn}{4\pi\lambda}\int_0^{2\pi}\int_0^{\pi/2}\int_{l_1}^{l_2}\left[\begin{array}{c} u(0) + (2d - r\cos\varphi)\left(\frac{du}{dz}|_{z=0}\right) \\ +\frac{1}{2}(2d - r\cos\varphi)^2\left(\frac{d^2u}{dz^2}|_{z=0}\right)\end{array}\right]\cos\varphi\sin\varphi\exp(-r/\lambda)\,drd\varphi d\omega. \tag{10}$$

The slip flow boundary condition can be obtained by equalizing the actual shear stress on the boundary with the shear stress predicted by the definition of ideal gas viscosity, as shown in the following equation:

$$\sigma\left(W_{up} + M_{up}\right) = \mu\left(\frac{du}{dz}|_{z=0}\right) = \frac{1}{3}nm\bar{v}\lambda\left(\frac{du}{dz}|_{z=0}\right). \tag{11}$$

Via the above equation, the "equivalent" second order slip flow boundary condition is shown in the following:

$$\begin{aligned} u = {} & \frac{2}{3}\lambda\frac{du}{dz}\frac{\left\{\begin{array}{c} 2-\sigma+\sigma(-1+2\sigma)K_N^{-3}Ei\left(-K_N^{-1}\right)+\sigma\exp\left(-K_N^{-1}\right)\left[(-1+2\sigma)K_N^{-2}+(1-2\sigma)K_N^{-1}+(-2+\sigma)\right] \\ -(4-4\sigma)K_N^{-3}Ei\left(-2K_N^{-1}\right)-\exp\left(-2K_N^{-1}\right)\left[(2-2\sigma)K_N^{-2}-(1-\sigma)K_N^{-1}+(1-\sigma)\right]\end{array}\right\}}{\sigma\left\{\begin{array}{c} 1+\sigma K_N^{-2}Ei\left(-K_N^{-1}\right)+\exp\left(-K_N^{-1}\right)\left[\sigma K_N^{-1}-\sigma\right] \\ +(4-4\sigma)K_N^{-2}Ei\left(-2K_N^{-1}\right)+\exp\left(-2K_N^{-1}\right)\left[(2-2\sigma)K_N^{-1}-(1-\sigma)\right]\end{array}\right\}} \\ & -\lambda^2\frac{d^2u}{dz^2}\frac{\left\{\begin{array}{c} 6+(-8+11\sigma)K_N^{-4}Ei\left(-K_N^{-1}\right)+\exp\left(-K_N^{-1}\right)\left[(-8+11\sigma)K_N^{-3}+(8-11\sigma)K_N^{-2}+(-16+10\sigma)K_N^{-1}-6\sigma\right] \\ +(16-16\sigma)K_N^{-4}Ei\left(-2K_N^{-1}\right)+\exp\left(-2K_N^{-1}\right)\left[(8-8\sigma)K_N^{-3}-(4-4\sigma)K_N^{-2}+(4-4\sigma)K_N^{-1}-(6-6\sigma)\right]\end{array}\right\}}{\left\{\begin{array}{c} 12+12\sigma K_N^{-2}Ei\left(-K_N^{-1}\right)+\exp\left(-K_N^{-1}\right)\left[12\sigma K_N^{-1}-12\sigma\right] \\ +(48-48\sigma)K_N^{-2}Ei\left(-2K_N^{-1}\right)+\exp\left(-2K_N^{-1}\right)\left[(24-24\sigma)K_N^{-1}-(12-12\sigma)\right]\end{array}\right\}}, \end{aligned} \tag{12}$$

where Ei is the exponential integral function. Compared with Equation (1), the parameter C_1 and C_2 of the proposed model can be readily determined.

The gas slippage boundary condition can be also expressed with boundary shear stress in the form of Equation (2). Here, because of the assumed laminar flow, the shear stress is a function of position (d in the derivation) and the viscosity satisfies the following relationship on planar surface:

$$\tau = \mu\left(\frac{du}{dz}\right). \tag{13}$$

Therefore, by comparing Equation (3) with Equation (12), A_1 and A_2 can be determined as

$$A_1 = \frac{2}{3}\frac{\left\{\begin{array}{c} 2-\sigma+\sigma(-1+2\sigma)K_N^{-3}Ei\left(-K_N^{-1}\right)+\sigma\exp\left(-K_N^{-1}\right)\left[(-1+2\sigma)K_N^{-2}+(1-2\sigma)K_N^{-1}+(-2+\sigma)\right] \\ -(4-4\sigma)K_N^{-3}Ei\left(-2K_N^{-1}\right)-\exp\left(-2K_N^{-1}\right)\left[(2-2\sigma)K_N^{-2}-(1-\sigma)K_N^{-1}+(1-\sigma)\right]\end{array}\right\}}{(2-\sigma)\left\{\begin{array}{c} 1+\sigma K_N^{-2}Ei\left(-K_N^{-1}\right)+\exp\left(-K_N^{-1}\right)\left[\sigma K_N^{-1}-\sigma\right] \\ +(4-4\sigma)K_N^{-2}Ei\left(-2K_N^{-1}\right)+\exp\left(-2K_N^{-1}\right)\left[(2-2\sigma)K_N^{-1}-(1-\sigma)\right]\end{array}\right\}}, \tag{14}$$

$$A_2 = \frac{\left\{\begin{array}{c} 6+(-8+11\sigma)K_N^{-4}Ei\left(-K_N^{-1}\right)+\exp\left(-K_N^{-1}\right)\left[(-8+11\sigma)K_N^{-3}+(8-11\sigma)K_N^{-2}+(-16+10\sigma)K_N^{-1}-6\sigma\right] \\ +(16-16\sigma)K_N^{-4}Ei\left(-2K_N^{-1}\right)+\exp\left(-2K_N^{-1}\right)\left[(8-8\sigma)K_N^{-3}-(4-4\sigma)K_N^{-2}+(4-4\sigma)K_N^{-1}-(6-6\sigma)\right]\end{array}\right\}}{\left\{\begin{array}{c} 12+12\sigma K_N^{-2}Ei\left(-K_N^{-1}\right)+\exp\left(-K_N^{-1}\right)\left[12\sigma K_N^{-1}-12\sigma\right] \\ +(48-48\sigma)K_N^{-2}Ei\left(-2K_N^{-1}\right)+\exp\left(-2K_N^{-1}\right)\left[(24-24\sigma)K_N^{-1}-(12-12\sigma)\right]\end{array}\right\}}. \tag{15}$$

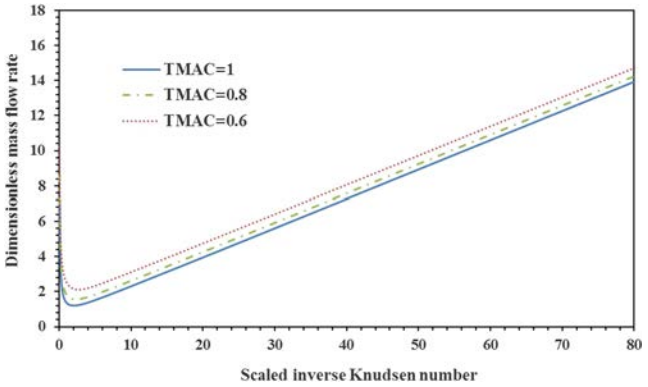

FIG. 4. Variation of dimensionless mass flow rate with respect to scaled inverse Knudsen number.

Using the proposed model, we can calculate the dimensionless mass flow rate Q_p as

$$Q_p = \frac{D}{6} + \frac{\sqrt{\pi}}{2}C_1 + \frac{\pi}{2D}C_2. \tag{16}$$

In the above equation, the scaled inverse Knudsen number D is defined as

$$D = \sqrt{\pi}\Big/(2K_N). \tag{17}$$

The variation of Q_p with respect to D with different TMAC is plotted in Figure 4, from which we can see that our model is able to capture the transition of the flow rate. As the TMAC increases, the "transition" Knudsen number also increases. The TMAC governs the degree of slippage at the surface and is affected by the roughness of the surface.[15] The value of this parameter is not measurable. It is commonly believed that TMAC falls between 0.6 and 1, as summarized by Ref. 1.

In the above model, we only consider two types of molecules: the molecules hits the upper wall after one molecular collision and the molecules directly impinge into the lower wall after one molecular collision. There are also molecules that hit the lower wall and upper wall multiple times. The momentum carried by these molecules is ignored. The reason we make this approximation is that the momentum loss rate is usually higher than 60%[1] (TMAC > 0.6). As such, after two times of wall collision, less than 16% = $(1-0.6)^2$ * 100% momentum is left with for the molecules. Consider the "long" distance these molecules will travel, and their quantity is also small (quantity decreases exponentially with respect to distance, as shown in Equation (3)). For Knudsen number up to 2, it can be estimated that the total momentum carried by molecules that have at least 2 times wall collision is less than 6% of *Type* 1 molecules. Therefore, the contribution of these molecules can be safely ignored in the current model, considering the target accuracy of the current model is 90%.

The mass transfer enhancement effect induced by gas slippage can be quantified by an "enhancement factor,"[1] as shown in the following equation:

$$S = 1 + 6C_1K_N + 12C_2K_N^2. \tag{18}$$

It can be seen that when Knudsen number is very small, the enhancement factor becomes 1 and the slippage effect disappears.

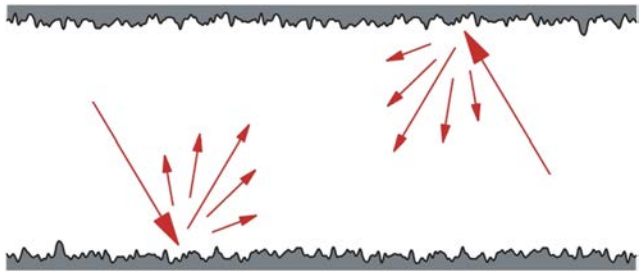

FIG. 5. Molecular interactions with a rough surface.

Variable rough surface

In this case, the surfaces are assumed planar with some roughness. Note that given a surface, specified in statistical terms, it is difficult to theoretically calculate the scattered field (also specified in statistical terms). The ratio of the number of diffuse reflections to that of all reflections is defined as the diffuse reflection ratio σ, varying from 0 to 1. Figure 5 shows complex molecular-wall interactions in the case of a rough surface. Following Refs. 16–18, the ratio of the number of diffuse reflections at a given impinge angle φ to that of all reflections from a single moderately rough surface is given by

$$\sigma(\varphi) = 1 - \exp\left[-(4\pi\cos\varphi\cdot\sigma_b/\lambda)^2\right], \tag{19}$$

where φ is the incident angle, σ_b is the root-mean-square surface roughness, and λ is the mean free path. It is important to note that using the mean free path in Equation (19) instead of wave length (as per original expression) is acceptable since they are of the same order for our problems. It can be seen from Equation (19) that, when σ_b approaches 0 (surface is perfectly smooth), $\sigma(\varphi)$ approaches 0 for all φ, meaning that no reflection is diffusive and no momentum is lost on the surface. On the other hand, when σ_b approaches infinity (surface is extremely rough), $\sigma(\varphi)$ approaches 1 for all φ, meaning that all reflection is diffusive.

In the case of rough surface, the momentum carried by these molecules can be computed as follows:

$$\bar{W}_{up} = \frac{\bar{\nu}mn}{4\pi\lambda}\int_0^{2\pi}\int_0^{\pi/2}\int_{l_1}^{l_2}\sigma(\varphi)\left(1-\sigma(\varphi)\right)u\left(2d-r\cos\varphi\right) \times\cos\varphi\sin\varphi\exp\left(-r/\lambda\right)drd\varphi d\omega, \tag{20}$$

$$\bar{M}_{up} = \frac{\bar{\nu}mn}{4\pi\lambda}\int_0^{2\pi}\int_0^{\pi/2}\int_0^{l_1}\sigma(\varphi)\,u\left(r\cos\varphi\right)\cos\varphi\sin\varphi \times\exp\left(-r/\lambda\right)drd\varphi d\omega. \tag{21}$$

The slip flow boundary condition can then be obtained similarly as that shown in Equation (11),

$$\bar{W}_{up} + \bar{M}_{up} = \mu\left(\frac{du}{dz}\Big|_{z=0}\right) = \frac{1}{3}nm\bar{\nu}\lambda\left(\frac{du}{dz}\Big|_{z=0}\right). \tag{22}$$

The solution of the above equation has no explicit formulation. Here, after simplification and order truncation, the slip boundary condition as a function of roughness factor can be approximately expressed as

$$u \approx \frac{2}{3}\lambda\frac{du}{dz}\frac{\left\{1+\exp\left(-R_D^2\right)+\exp\left(-K_N^{-1}\right)\left[\left(1-3\exp\left(-R_D^2\right)\right)K_N^{-2}-\left[1-3\exp\left(-R_D^2\right)\right]K_N^{-1}-1\right]\right\}}{\left\{\left[1-\exp\left(-R_D^2\right)\right]+\exp\left(-K_N^{-1}\right)\left[\left[1-2\exp\left(-R_D^2\right)\right]K_N^{-1}-\left[1-2\exp\left(-R_D^2\right)\right]\right]\right\}}$$

$$-\lambda^2\frac{d^2u}{dz^2}\frac{\left\{6+\exp\left(-K_N^{-1}\right)\left[\begin{array}{c}\left[3-11\exp\left(-R_D^2\right)\right]K_N^{-3}+\left[-3+11\exp\left(-R_D^2\right)\right]K_N^{-2}\\+\left[-6-10\exp\left(-R_D^2\right)\right]K_N^{-1}-6\left[1-\exp\left(-R_D^2\right)\right]\end{array}\right]\right\}}{\left\{12+\exp\left(-K_N^{-1}\right)\left[12\left[1-\exp\left(-R_D^2\right)\right]K_N^{-1}-12\left[1-\exp\left(-R_D^2\right)\right]\right]\right\}}. \quad (23)$$

In the above equation, we have introduced a dimensionless number R_D as

$$R_D = 4\pi\sigma_b/\lambda, \quad (24)$$

where R_D is calculated from the ratio between the surface roughness and the mean free path. In other words, it denotes the "level" of the curvature with respect to the free movement of the gas molecules. We use the inverse of the enhancement factor S in Equation (18) to show the effect of surface roughness on gas slippage. The variation of $1/S$ with respect to the Knudsen number from 0.001 to 1 for different R_D is shown in Figure 6. According to Figure 6, when R_D increases from 0.01 to 10, the enhancement effect also increases, which means that when the surface becomes rougher, more momentum is lost on the surface, and the slippage effect is thus larger. When R_D approaches 0, the surface approaches being perfectly smooth surface and the slippage effect disappears, as shown by the R_D = 0.01 line in Figure 6.

The investigation of the surface roughness on the gas slippage phenomena fundamentally reveals the origin of the momentum loss effect. The study also extends our proposed model to more complex geometry, as the geometry in a "local" scale can be viewed as the curvature of the surface.

MODEL VALIDATION

Molecular simulation data

In this section, we use both numerical simulation results as well as physical experimental data to validate our model. The chosen numerical simulation results we choose are from the work of Guo *et al.*[19] (after Li *et al.*[20]), while the experimental data are from the work of Colin *et al.*[21] and Maurer *et al.*[22]

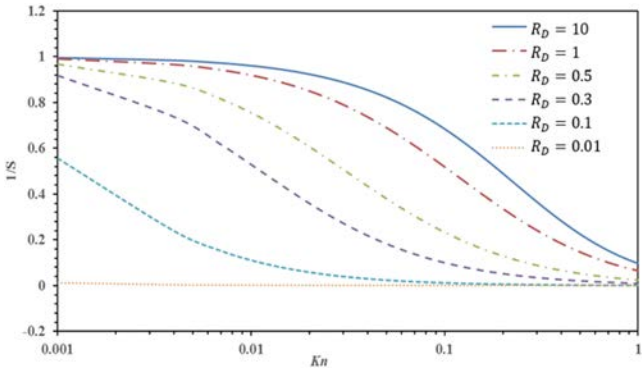

FIG. 6. Variation of $1/S$ with respect to Knudsen number for different R_D.

We compare our model against the benchmark data along with four existing models, developed by Wu,[3] Hadjiconstantinou,[23] Pan,[24] and Aubert and Colin,[25] respectively. Wu's model is derived using kinetic approach. Hadjiconstantinou's model is modified from Cercignani's model, which is a solution of linearized Boltzmann equation. Pan's model is an empirical first-order model, obtained by fitting the results of DSMC simulation.[26] The model of Aubert and Colin is obtained from an extended version of Navier-Stokes (NS) equation based on Deissler's work.[27] The slippage coefficients of the four models are listed in Table I, where C_1 and C_2 refer to Equation (1). According to Ref. 1, the model of Aubert and Colin and Wu's model are among the most accurate non-empirical models.

The work of Guo *et al.*[19] is based on the Lattice Boltzmann Method (LBM) with purely diffusive reflection (TMAC = 1). It is a generalized version of Lattice Boltzmann Method with kinetic bounce-back boundary. The results of Guo *et al.* have been compared with experimental data[19,20] and have shown sound accuracy with Knudsen number up to 10. In this paper, we compare the dimensionless mass flow rate Q with that predicted by the LBM method. Q is defined as

$$Q = -\int_0^h \rho u dz\sqrt{2RT}/\left(h^2\partial p/\partial x\right) \quad (25)$$

(The flow rate formulation based on our model can be explicitly expressed and is shown in Equation (16)). The comparison is shown in Figure 7, from which we can see that when Knudsen number is smaller than 2, the difference between our kinetic model and the LBM model is on average less than 10%. The minimum value of Q predicted by our model occurs at $K_N \approx 0.4$, while the minimal Q is at $K_N \approx 0.8$ according to the LBM results. When the Knudsen number is larger than 2, our model is less accurate. The result is due to the limitation of the kinetic model. In the kinetic model we use, it is assumed that probability of gas molecular collision is uniform with respect to all directions. Based on this assumption, the probability that a gas molecular hits another molecular increases exponentially as the distance it travels increases, as shown in Equation (3). When Knudsen number exceeds a certain level, the gas molecules will frequently hit the wall and molecular-molecular collisions become non-uniform. As such, the assumption of the kinetic model becomes invalid at relatively higher Knudsen number. Therefore, the application of our proposed model should be restricted to low to moderate Knudsen number, smaller than 2.

TABLE I. List of slippage coefficients of the models for comparison.

Model	C1	C2	Approach
Hadjiconstantinou[23]	1.11	0.61	Boltzmann equation
Pan[24]	1.1254	...	DSMC
Aubert and Colin[25]	$\frac{2-\sigma}{\sigma}$	$\frac{9}{8}$	N-S equation
Wu[3]	$\frac{2}{3}\left[\frac{3-\sigma f_W^3}{\sigma}-\frac{9\left(1-f_W^2\right)}{2K_N}\right]$	$\frac{1}{4}\left[f_W^4+\frac{2}{K_N^2}\left(1-f_W^2\right)\right]$	Kinetic derivation $f_W=\min\left[\frac{1}{K_N},1\right]$

For the other four models used for comparison, Wu's model is in general acceptable. The change of trend at $K_N = 1$ in Wu's results is because of the selection of parameter f in his formulation, as shown in Table I.

Pan's first order model and the model Aubert and Colin show significant dispatch with the benchmark data when Knudsen number is relatively high. Hadjiconstantinou's model is accurate for $K_N < 0.5$, which is also reported by Refs. 8 and 23.

Physical experimental data

The two sets of experimental data in Refs. 21 and 22 are used by Ref. 1 for comparison among several gas slippage conditions. The flow enhancement factor S used for comparison is defined in Equation (18). Both of the two experiments are chip-flooding experiments.

In Colin's experiment, the TMAC is 0.93, obtained by fitting the enhancement factor using Ref. 27's second-order boundary condition. Maurer's experiment is with helium. The TMAC is 0.91 ± 0.03, obtained by data fitting with a second-order velocity boundary condition.

The comparison with the four models against Colin's data is shown in Figure 8, from which we can see that our results match the experimental data very well. The comparison against Maurer's data is shown in Figure 9. As shown by Figure 9, the results predicted by our model are in average within 10% difference with Maurer's experimental data, which is within the scatter of the experiment results, as reported by Ref. 22. All the other four models demonstrate obvious disparity with the two sets of experimental data. Pan's first-order boundary condition, which matches Colin's data pretty well, has huge disparity with Maurer's data when the Knudsen number is greater than 0.5, indicating the limitation of the first-order boundary condition in handling moderate Knudsen number.

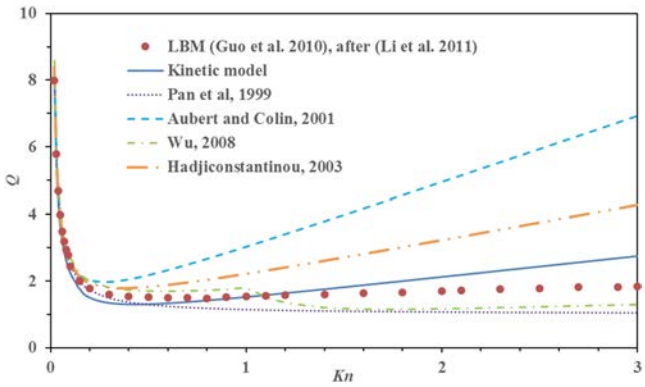

FIG. 7. Comparison of the flow rate between our model and Lattice Boltzmann method.[18] The data are collected from Ref. 19. TMAC = 1.

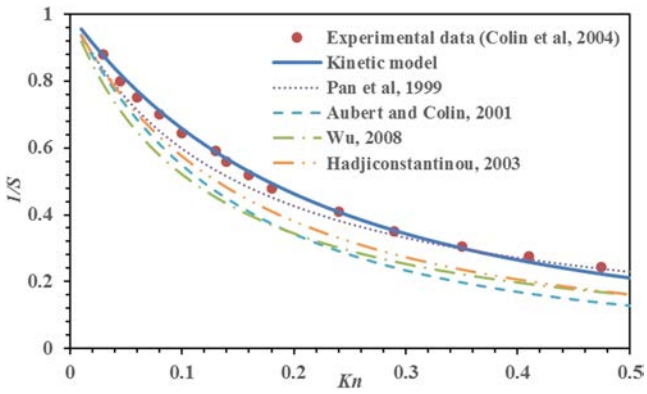

FIG. 8. Comparison of the inverse flux enhance factor between theoretical models with experimental data from Ref. 21. After Ref. 1. TMAC = 0.93.

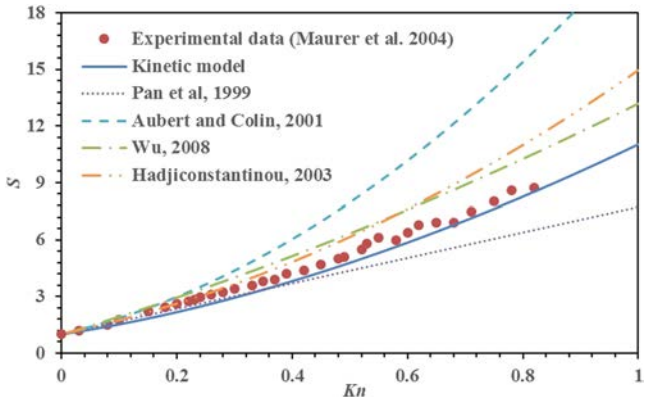

FIG. 9. Comparison of the flux enhance factor between theoretical models with experimental data from Ref. 22. After Ref. 1. TMAC = 0.91.

DISCUSSION AND CONCLUSION

The question of slip flow boundary condition has received significant attention in the research community. To investigate and quantify the issue, a single-phase/single-component gas flow within micro- and nano-flow channels is considered in this paper. An "equivalent" second order slip flow is proposed, basing on kinetic theory of gases. The comparison with numerical and physical experimental results shows the validity of the selected approach. The model has sound accuracy with low to moderate Knudsen number. The proposed model is

fully based on the kinetic theory of gases, containing minimum fitting parameters.

The influence of the TMAC on the mass flow rate is also analyzed. Meanwhile, the impact of surface roughness on the slippage effect is also investigated, which not only fundamentally reveals the origin of momentum loss but also extends the model to cases where surface has complex curvatures. The model is also applicable to study shale-specific transport properties.[28]

For flow with Knudsen number higher than 2, our model fails to match the benchmark data. This is because that when Knudsen number is higher than a certain level, the fundamental assumptions to calculate the collision probability and free movement distance become invalid. In this sense, we restrict the application of our model to Knudsen number smaller than 2. Besides, another limitation of our model is that it can only be applied to steady or near-steady flow.

To sum up, we have proposed an accurate non-empirical gas slippage model. The model is accurate for low to moderate Knudsen number and can be conveniently applied to many engineering areas.

ACKNOWLEDGMENTS

The author would like to thank Dr. Guangping Xu and Dr. Xiaolong Yin for inspiring discussions.

APPENDIX A: BASIC CONCEPTS OF THE KINETIC MODEL

The Knudsen number is defined as

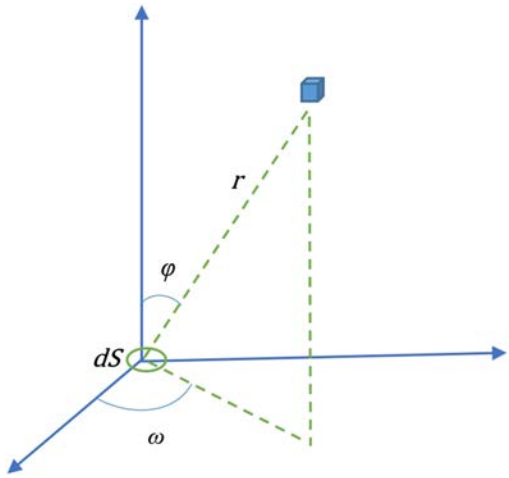

FIG. 10. Coordinate system showing element of area dS of the wall and element of volume $d\tau$ of the gas.

$$K_N = \frac{\lambda}{d}, \tag{A1}$$

where λ is the mean free path of gas and d is the diameter of the mirco-channel, and λ can be calculated based on the kinetic theory as

$$\lambda = \frac{k_B T}{\sqrt{2}\pi d^2 P}. \tag{A2}$$

In the above equation, k_B is the Boltzmann constant, T is the temperature, and P is the pressure. In this work, we assume the gas flow is under isothermal condition, neglecting the thermal creep effect; therefore, the temperature is set to be constant.

The coordinate system of the kinetic model is shown in Figure 10.

APPENDIX B: DETAILED FORMULATION OF THE MOMENTUM FORMULATION

$$\begin{aligned} M_{up} = {} & \frac{\bar{v}mn}{48}\lambda^2\frac{d^2u}{dz^2}\left\{6 + 3K_N^{-4}Ei\left(-K_N^{-1}\right) - \exp\left(-K_N^{-1}\right)\left[-3K_N^{-3} + 3K_N^{-2} + 6K_N^{-1} + 6\right]\right\} \\ & \cdots + \frac{\bar{v}mn}{48}\lambda\frac{du}{dz}\left\{8 + 8K_N^{-3}Ei\left(-K_N^{-1}\right) + \exp\left(-K_N^{-1}\right)\left[8K_N^{-2} - 8K_N^{-1} - 8\right]\right\} \\ & \cdots + \frac{\bar{v}mn}{48}u\left\{12 + 12K_N^{-2}Ei\left(-K_N^{-1}\right) + \exp\left(-K_N^{-1}\right)\left[12K_N^{-1} - 12\right]\right\}, \end{aligned} \tag{B1}$$

$$\begin{aligned} W_{up} = {} & (1-\sigma)\frac{\bar{v}mn}{48}\lambda^2\frac{d^2u}{dz^2}\left\{-11K_N^{-4}Ei\left(-K_N^{-1}\right) + \exp\left(-K_N^{-1}\right)\left[-11K_N^{-3} + 11K_N^{-2} - 10K_N^{-1} + 6\right]\right\} \\ & \cdots + (1-\sigma)\frac{\bar{v}mn}{48}\lambda\frac{du}{dz}\left\{-16K_N^{-3}Ei\left(-K_N^{-1}\right) - \exp\left(-K_N^{-1}\right)\left[16K_N^{-2} - 16K_N^{-1} + 8\right]\right\} \\ & \cdots + (1-\sigma)\frac{\bar{v}mn}{48}u\left\{-12K_N^{-2}Ei\left(-K_N^{-1}\right) + \exp\left(-K_N^{-1}\right)\left[-12K_N^{-1} + 12\right]\right\} \\ & \cdots + (1-\sigma)\frac{\bar{v}mn}{48}\lambda^2\frac{d^2u}{dz^2}\left\{16K_N^{-4}Ei\left(-2K_N^{-1}\right) - \exp\left(-2K_N^{-1}\right)\left[-8K_N^{-3} + 4K_N^{-2} - 4K_N^{-1} + 6\right]\right\} \\ & \cdots + (1-\sigma)\frac{\bar{v}mn}{48}\lambda\frac{du}{dz}\left\{32K_N^{-3}Ei\left(-2K_N^{-1}\right) + \exp\left(-2K_N^{-1}\right)\left[16K_N^{-2} - 8K_N^{-1} + 8\right]\right\} \\ & \cdots + (1-\sigma)\frac{\bar{v}mn}{48}u\left\{48K_N^{-2}Ei\left(-2K_N^{-1}\right) + \exp\left(-2K_N^{-1}\right)\left[24K_N^{-1} - 12\right]\right\}. \end{aligned} \tag{B2}$$

[1]W. M. Zhang, G. Meng, and X. Wei, "A review on slip models for gas microflows," Microfluid. Nanofluid. **13**(6), 845 (2012).
[2]B. Y. Cao, J. Sun, M. Chen, and Z. Y. Guo, "Molecular momentum transport at fluid-solid interfaces in MEMS/NEMS: A review," Int. J. Mol. Sci. **10**(11), 4638–4706 (2009).
[3]L. Wu, "A slip model for rarefied gas flows at arbitrary Knudsen number," Appl. Phys. Lett. **93**(25), 1 (2008).
[4]Y. Sone, "Asymptotic theory of flow of rarefied gas over a smooth boundary I," in *Rarefied Gas Dynamics*, edited by L. Trilling and H. Y. Wachman (Academic Press, New York, 1969), pp. 243–253.
[5]A. Dinler, R. W. Barber, D. R. Emerson, S. K. Stefanov, and K. Orucoglu, "On the degree of boundary slip over nonplanar surfaces," Microfluid. Nanofluid. **15**(6), 807 (2013).
[6]A. Dinler, R. W. Barber, D. R. Emerson, S. K. Stefanov, and K. Orucoglu, "Role of surface shape on boundary slip and velocity defect," Phys. Rev. E **86**(1), 016314 (2012).
[7]N. G. Hadjiconstantinou, "Validation of a second-order slip model for dilute gas flows," Microscale Thermophys. Eng. **9**(2), 137–153 (2005).
[8]H. Xue, Q. Fan, and C. Shu, "Prediction of micro-channel flows using direct simulation Monte Carlo," Probab. Eng. Mech. **15**(2), 213 (2000).
[9]X. Nie, G. D. Doolen, and S. Chen, "Lattice-boltzmann simulations of fluid flows in MEMS," J. Stat. Phys. **107**(1/2), 279 (2002).
[10]T. Ohwada and K. Xu, "The kinetic scheme for the full- equations," J. Comput. Phys. **201**(1), 315 (2004).
[11]F. Javadpour, "Nanopores and apparent permeability of gas flow in mudrocks (shales and siltstone)," J. Can. Pet. Technol. **48**(08), 16 (2009).
[12]C. Ho and Y. Tai, "Micro-electro-mechanical-systems (MEMS) and fluid flows," Annu. Rev. Fluid Mech. **30**, 579 (1998).
[13]W. G. Pollard and R. D. Present, "On gaseous self-diffusion in long capillary tubes," Phys. Rev. **73**(7), 762 (1948).
[14]R. D. Present, *Kinetic Theory of Gases* (McGraw-Hill, 1958), Vol. 222.
[15]C. Kleinstreuer and J. Koo, "Computational analysis of wall roughness effects for liquid flow in micro-conduits," J. Fluids Eng. **126**(1), 1 (2004).
[16]H. Davies, "The reflection of electromagnetic waves from a rough surface," Proc. IEE. **101**(7), 209–214 (1954).
[17]H. E. Bennett and J. O. Porteus, "Relation between surface roughness and specular reflectance at normal incidence," J. Opt. Soc. Am. **51**(2), 123–129 (1961).
[18]J. E. Harvey, S. Schröder, N. Choi, and A. Duparré, "Total integrated scatter from surfaces with arbitrary roughness, correlation widths, and incident angles," Opt. Eng. **51**(1), 013402 (2012).
[19]Z. Guo, C. Zheng, and B. Shi, "Lattice Boltzmann equation with multiple effective relaxation times for gaseous microscale flow," Phys. Rev. E **77**(3), 036707 (2008).
[20]Q. Li, Y. L. He, G. H. Tang, and W. Q. Tao, "Lattice Boltzmann modeling of microchannel flows in the transition flow regime," Microfluid. Nanofluid. **10**(3), 607–618 (2011).
[21]S. Colin, P. Lalonde, and R. Caen, "Validation of a second-order slip flow model in rectangular microchannels," Heat Transfer Eng. **25**(3), 23 (2004).
[22]J. Maurer, P. Tabeling, and P. Joseph, "Second-order slip laws in microchannels for helium and nitrogen," Phys. Fluids **15**(9), 2613 (2003).
[23]N. G. Hadjiconstantinou, "Comment on 's second-order slip coefficient," Phys. Fluids **15**(8), 2352–2354 (2003).
[24]L. S. Pan, G. R. Liu, and K. Y. Lam, "Determination of slip coefficient for rarefied gas flows using direct simulation Monte Carlo," J. Micromech. Microeng. **9**(1), 89 (1999).
[25]C. Aubert and S. Colin, "High-order boundary conditions for gaseous flows in rectangular microducts," Microscale Thermophys. Eng. **5**(1), 41 (2001).
[26]C. Cercignani, "Higher order slip according to the linearized Boltzmann equation," Institute of Engineering Research Report No. AS64 19, University of California, Berkeley, 1964.
[27]R. Deissler, "An analysis of second-order slip flow and temperature-jump boundary conditions for rarefied gases," Int. J. Heat Mass Transfer **7**(6), 681 (1964).
[28]L. Wang, S. Wang, R. Zhang, C. Wang, Y. Xiong, X. Zheng, S. Li, K. Jin, and Z. Rui, "Review of multi-scale and multi-physical simulation technologies for shale and tight gas reservoirs," J. Nat. Gas Sci. Eng. **37**, 560 (2017).